STEM CELLS®

TISSUE-SPECIFIC STEM CELLS

Mesenchymal Stem Cells Pretreated with Delivered Hph-1-Hsp70 Protein Are Protected from Hypoxia-Mediated Cell Death and Rescue Heart Functions from Myocardial Injury

WOOCHUL CHANG,[a] BYEONG-WOOK SONG,[b,c] SOYEON LIM,[d] HEESANG SONG,[e] CHI YOUNG SHIM,[f] MIN-JI CHA,[b,c] DONG HYUCK AHN,[g] YOUNG-GOOK JUNG,[g] DONG-HO LEE,[h] JI HYUNG CHUNG,[i] KI-DOO CHOI,[h] SEUNG-KYOU LEE,[h] NAMSIK CHUNG,[b,f] SANG-KYOU LEE,[g] YANGSOO JANG,[b,f] KI-CHUL HWANG[b]

[a]Department of Pharmacology, Yale University School of Medicine, New Haven, Connecticut, USA; [b]Cardiovascular Research Institute, Yonsei University College of Medicine, Seoul, Republic of Korea, [c]Brain Korea 21 Project for Medical Science, Yonsei University College of Medicine, Seoul, Republic of Korea, [d]Cardiovascular Research Institute, University of Rochester School of Medicine and Dentistry, Rochester, New York, USA; [e]Department of Pediatrics, Washington University in St. Louis School of Medicine, St. Louis, Missouri, USA; [f]Cardiology Division, Yonsei University College of Medicine, Seoul, Republic of Korea; [g]Department of Biotechnology, College of Life Science and Biotechnology, Yonsei University, Seoul, Republic of Korea; [h]ForHumanTech Co., Ltd, Hwa-Sung, Republic of Korea; [i]Severance Hospital Integration, Research Institute for Cerebral & Cardiovascular Diseases, Severance Hospital, 250 Seongsanno, Seodaemun-gu, Seoul, Republic of Korea

Key Words. Mesenchymal stem cells • Protein transduction domains • Myocardial infarction

ABSTRACT

Mesenchymal stem cell (MSC) therapy for myocardial injury has inherent limitations due to the poor viability of MSCs after cell transplantation. In this study, we directly delivered Hsp70, a protein with protective functions against stress, into MSCs, using the Hph-1 protein transduction domain ex vivo for high transfection efficiency and low cytotoxicity. Compared to control MSCs in in vitro hypoxic conditions, MSCs delivered with Hph-1-Hsp70 (Hph-1-Hsp70-MSCs) displayed higher viability and anti-apoptotic properties, including Bcl2 increase, reduction of Bax, JNK phosphorylation and caspase-3 activity. Hsp70 delivery also attenuated cellular ATP-depleting stress. Eight animals per group were used for in vivo experiments after occlusion of the left coronary artery. Transplantation of Hph-1-Hsp70-MSCs led to a decrease in the fibrotic heart area, and significantly reduced the apoptotic positive index by 19.5 ± 2%, compared to no-treatment controls. Hph-1-Hsp70-MSCs were well-integrated into the infarcted host myocardium. The mean microvessel count per field in the infarcted myocardium of the Hph-1-Hsp70-MSC-treated group (122.1 ± 13.5) increased relative to the MSC-treated group (75.9 ± 10.4). By echocardiography, transplantation of Hph-1-Hsp70-MSCs resulted in additional increases in heart function, compared to the MSCs-transplanted group. Our results may help formulate better clinical strategies for in vivo MSC cell therapy for myocardial damage. STEM CELLS *2009;27:2283–2292*

Disclosure of potential conflicts of interest is found at the end of this article.

INTRODUCTION

Mesenchymal stem cells (MSCs) show therapeutic potential for repair of myocardial infarctions and prevention of post-infarct congestive heart failure. MSCs produce a variety of cardio-protective signaling molecules, and have the ability to differentiate into both myocyte and vascular cell lineages after transplantation into the infarcted heart [1, 2]. However, poor viability of transplanted cells is a major limiting factor of cell therapy. Toma et al. [3] reported a very low survival rate (<1%) for MSCs transplanted into uninjured mouse hearts at 4 days after transplantation.

Heat shock proteins (Hsps) provide a defense against stress caused by high temperature, oxidative stress, pressure overload, and hypoxia/ischemia [4, 5]. A number of protective functions have been attributed to Hsps, especially Hsp70, including ion channel repair, redox balance restoration,

Author contributions: W.C., B.-W.S., S.L., H.S., C.Y.S., and J.H.C.: data collection and/or assembly of data, data analysis and interpretation; M.-J.C., D.H.A., Y.-G.J., D.-H.L., K.-D.C., and S.-K.L.: provision of study material, data interpretation; N.C., S.-K. L., and Y.J.: data interpretation, final approval of manuscript; K.-C.H.: conception and design, financial support, data analysis and interpretation, manuscript writing, final approval of manuscript. W.C. and B.-W.S. contributed equally to this work.

Correspondence: Ki-Chul Hwang, Ph.D., Cardiovascular Research Institute, Yonsei University College of Medicine, 250 Seongsanno, Seodaemun-gu, Seoul, 120-752, Korea. Telephone: 82-2-2228-8523; Fax: 82-2-365-1878; e-mail: kchwang@yuhs.ac; or Yangsoo Jang, M.D., Ph.D., Cardiology Division, Yonsei University College of Medicine, 250 Seongsanno, Seodaemun-gu, Seoul, 120-752, Korea. Telephone: 82-2-2228-8445; Fax: 82-2-365-1878; e-mail: jangys1212@yuhs.ac; or Sang-Kyou Lee, Ph.D., Department of Biotechnology, College of Life Science and Biotechnology, Yonsei University, Seoul, 120-749, Republic of Korea. Telephone: 82-2-2123-2889; Fax; 82-2-362-7265; e-mail: sjrlee@yonsei.ac.kr Received February 16, 2009; accepted for publication June 5, 2009; first published online in STEM CELLS *EXPRESS* June 18, 2009. 1066-5099/2009/$30.00/0 doi: 10.1002/stem.153

interaction with the nitric oxide-induced protection pathway, inhibition of proinflammatory cytokines, and preventing activation of the apoptosis pathway [6–11]. Although MSCs transfected with an anti-apoptotic gene using a retroviral vector enhanced their therapeutic effectiveness, constitutive expression of anti-apoptotic genes in MSCs may induce tumorigenesis, thereby altering their differentiation capacity and limiting their clinical application to humans [12–14]. Various challenges are presented by gene therapy procedures and genetic manipulation of MSCs using transfection, viral vectors or microinjection of proteins into cells. These include low transfection efficiency, cytotoxicity associated with chemical agents, and harmful retroviral transfection [15–17]. In order to overcome these problems, Protein Transduction Domains (PTDs), synthesized or identified in proteins from various species, have been shown to deliver therapeutic proteins with almost 100% efficiency into eukaryotic cells both in vitro and in vivo. In particular, a novel, cell-permeable PTD was identified from the human transcriptional factor Hph-1. The Hph-1-PTD has been successfully used to deliver immunosuppressive proteins in vivo and in vitro for the treatment of various autoimmune diseases through different administration routes [18]. In this study, Hsp70 was directly delivered into MSCs using Hph-1-PTD ex vivo. The protective effect of Hph-1-Hsp70 on MSCs from hypoxia-induced apoptosis and the in vivo therapeutic potential of Hph-1-Hsp70-treated MSCs were examined in myocardial infarction-induced rats.

Materials and Methods

Isolation and Culture of MSCs

MSCs were isolated and cultured from the femoral and tibial bones of donor rats [19]. Bone marrow-derived MSCs were collected from aspirates of the femurs and tibias of 4-week-old Sprague-Dawley male rats (about 100 g) with 10 ml of MSC medium consisting of Dulbecco's modified Eagle's medium (DMEM)-low glucose supplemented with 10% fetal bovine serum (FBS) and 1% antibiotic-penicillin and streptomycin solution. Flushed media were centrifuged at 1,600 rpm, 5 minutes and resuspended in serum-supplemented medium, and loaded onto a Percoll density gradient before centrifugation at 1,600 rpm, 30 minutes. Mononuclear cells recovered from the middle interface were washed twice, resuspended in 10% FBS-DMEM, and plated at 1×10^6 cells/100 cm^2 in flasks. Cultures were maintained at 37°C in a humidified atmosphere containing 5% CO_2. After 48 or 72 hours, nonadherent cells were discarded, and the adherent cells were thoroughly washed twice with phosphate-buffered saline (PBS). Fresh complete medium was added and replaced every 3 or 4 days for 10 days. To further purify the MSCs, the Isolex Magnetic Cell Selection System (Baxter Healthcare Corporation, Irvine, CA, http://www.baxter.com) was used. Briefly, cells were incubated with M-450 Dynabeads coated with anti-CD34 monoclonal antibody. A magnetic field was applied to the chamber and the $CD34^+$ cell-bead complexes were separated magnetically from the remaining cell suspension, for further culturing of the $CD34^-$ fraction. Cells were harvested after incubation with 0.25% trypsin and 1 mM EDTA for 5 minutes at 37°C, replated in 1×10^5/100-cm^2 plates, and grown for approximately 10 days. The characteristics of MSCs were demonstrated by immunophenotyping. To verify the nature of cultured MSCs, cells were labeled for various surface and intracellular markers, and analyzed by flow cytometry. Cells were harvested, washed with PBS, and labeled with antibodies against CD14, CD34, CD71, CD90, CD105 or ICAM-1 conjugated with fluorescein isothiocyanate (FITC) or Texas red. FITC-conjugated goat anti-mouse IgG and Texas red-conjugated goat anti-rabbit IgG from Jackson Immunoresearch Laboratories (West Grove, PA, USA, http://www.jacksonimmuno.com) were used as secondary antibodies. Labeled cells were assayed by flow cytometry and analyzed with CellQuest Pro Software (BectonDickinson, San Jose, CA, http://www.bd.com).

Protein Purification of Hph-1-Hsp70

The expression plasmid pHph-1-Hsp70 was transformed by heat shock into BL21-DE3 (ATCC N. 53863). Transformed bacteria were grown at to OD_{600} 0.7 in LB medium. Protein expression was induced at 37°C with 1 mM IPTG (Gibco BRL, Grand Island, NY, http://www.invitrogen.com) for 4 hours. Cells were harvested by centrifugation at 6,000 rpm for 20 minutes and the pellet was resuspended in binding buffer (50 mM NaH_2PO_4, 300 mM NaCl, 10 mM Imidazole, pH 8.0). Bacteria were sonicated 6 seconds on/off for a total time of 8 minutes (Heat systems, ultrasonic processor XL). After removal of the cell debris by centrifugation, 0.5 ml of 50% Ni^{2+}-NTA agarose beads (Qiagen, Hilden, Germany, http://www1.qiagen.com) was added to the clarified cell extract. Agarose bead binding was performed at 4°C and the extract was loaded on to poly-Prep chromatography columns (0.8 × 4, Bio-Rad Laboratories, Richmond, CA, USA, http://www.bio-rad.com). Columns were washed with wash buffer (20 mM Tris-HCl, 500 mM NaCl, 20 mM Imidazole, pH 7.9) and eluted with 1 ml of elution buffer one (50 mM NaH_2PO_4, 300 mM NaCl, 250 mM Imidazole, pH 8.0) and elution buffer two (50 mM NaH_2PO_4, 300 mM NaCl, 500 mM Imidazole, pH 8.0), followed by passage through a PD-10 desalting column (Amersham Pharmacia Biotech, Tokyo, Japan, http://www1.gelifesciences.com).

Hsp70 Delivery into MSCs and Experimental Hypoxia

MSCs were cultured at 80% confluency and 0.5 μM Hph-1-Hsp70 was added to the cell culture for 1-hour, followed by incubation in hypoxic conditions for 24 hours. Media used under hypoxic conditions was 1% FBS-DMEM containing antibiotics (100 U/ml penicillin and 100 μg/ml streptomycin), which was degassed and substituted with a gas mixture of 10% CO_2, 5% H_2, and 85% N_2. The airtight humidified hypoxic chamber (Anaerobic Environment, ThermoForma, Marietta, OH, USA, http://www.thermo.com) was maintained at 37°C and continuously gassed with N_2.

Cell Survival

Cell survival was measured with the PreMix WST-1 Cell Counting System (TAKARA BIO Inc., Shiga, Japan, http://www.takara-bio.com), which uses a colorimetric assay for cleavage of the red tetrazolium salt (WST-1) by mitochondrial succinate-tetrazolium reductase in viable cells. An increase in enzyme activity increases the production of formazan dye, and so the quantity of dye is related directly to the number of metabolically active cells. Cells (2×10^4) were seeded into wells of a 96-well culture plate and incubated under hypoxic conditions after pretreatment with or without Hph1-Hsp70. WST-1 cell counting reagent was added directly to the supernatant (10 μl/100 μl growth medium), and incubated at 37°C for 3 hours. Absorbancy of the solubilized dark red formazan product was determined at 450 nm.

Caspase-3 Activity Assay

MSCs (1×10^6) were treated with Hph1-Hsp70 and incubated at 37°C for 1-hour before inducing apoptosis by exposure to hypoxic conditions for 24 hours at 37°C. Cells were harvested, and lysates were evaluated for caspase activity with ApopTarget™ Capase-3 (BioSource International Inc., Grand Island, NY, http://www.invitrogen.com) according to the manufacturer's instructions. This assay is based on the generation of free DEVD-*p*NA chromophores when the provided substrate is cleaved by caspase-3. Upon substrate cleavage, free *p*NA light absorbance was quantified using a microplate reader at 405 nm.

Assay of Intracellular ATP Levels

Cellular ATP levels were measured using a commercial luciferase kit, ViaLight HS (Cambrex, Walkersville, MD, USA, http://www.cambrex.com) according to the manufacturer's instructions. Briefly, 2×10^4 cells were plated in 96-well luminescence-compatible plates. Cells were pretreated with or without Hph1-Hsp70 fusion protein for 1-hour and incubated under hypoxic conditions for 24 hours. The culture plate was removed from the incubator and cooled at room temperature for at least 5 minutes, after which 100 μl of Nucleotide Releasing Reagent was added to each well. After at least 5 minutes, 20 μl of ATP monitoring reagent was added to each well and the plate was read immediately. Luminescence was measured by a LS 50B luminometer (Perkin-Elmer Life and Analytical Sciences, Boston, MA, USA, http://www.perkinelmer.com).

Immunoblot Analysis

Proteins were separated by 10–12% SDS-PAGE and electrotransferred to methanol-treated polyvinylidene diflouride membranes. Membranes were blocked with 5% nonfat dried milk in PBS. After 1-hour at room temperature, membranes were probed overnight at 4°C with mouse polyclonal antibodies against Hsp70, phospho-JNK, c-Jun N-terminal kinase (JNK), Bcl-2 or Bax (Santa Cruz Biotechnology, Santa Cruz, CA, http://www.scbt.com) followed by IgG-peroxidase as secondary antibody. Blots were developed using enhanced chemiluminescence kits (ECL, Amersham Pharmasia Biotech, Tokyo, Japan).

Measurement of Apoptosis by Annexin V Staining

Cells were trypsinized and gently washed with serum-containing culture medium and PBS, before resuspension in binding buffer (10 mM HEPES, 140 mM NaCl, 25 mM $CaCl_2$) and incubation with annexin V-FITC (BD Pharmingen, San Diego, CA, http://www.bdbiosciences.com/index_us.shtml) and propidium iodide (PI; Sigma, St. Louis, MO, http://www.sigma.com) at room temperature for 15 minutes. Fluorescence analysis was carried out using a flow cytometer (Beckman Coulter, Inc., San Diego, CA, http://www.beckmancoulter.com). In all data included in this study, forward scatter/side scatter (FSC/SSC) distribution pattern of cells was detected and analyzed. Annexin V-FITC signals were detected using an FL1 detector and PI signals were detected using an FL3 detector.

Induction of Myocardial Infarction

Experiments were conducted in accordance with the International Guide for the Care and Use of Laboratory Animals. The protocol was approved by the Animal Research Committee of the Yonsei University College of Medicine. Under general anesthesia, 8-week-old Sprague-Dawley male rats (about 250 g) were intubated, and positive-pressure ventilation (180 ml/minute) was maintained with room air supplemented with oxygen (2 l/minute) using a Harvard ventilator. The heart was exposed through a 2-cm left lateral thoracotomy. The pericardium was incised and a 6-0 silk suture (Johnson & Johnson, Langhome, PA, http://www.jnj.com) was placed around the proximal portion of the left coronary artery, beneath the left atrial appendage. Ligature ends were passed through a small length of plastic tube to form a snare. For coronary artery occlusion, the snare was pressed onto the surface of the heart directly above the coronary artery and a hemostat applied to the snare. Ischemia was confirmed by the blanching of the myocardium and dyskinesis of the ischemic region. After 60 minutes of occlusion, the hemostat was removed and the snare released for reperfusion, with the ligature left loose on the surface of the heart. Restoration of normal rubor indicated successful reperfusion. Wounds were sutured and the thorax was closed under negative pressure. Rats were weaned from mechanical ventilation and returned to cages to recover. In sham-operated rats, the same procedure was executed without tightening the snare (normal).

MSCs Labeling and Transplantation

MSCs were labeled with DAPI to determine cell viability by adding sterile DAPI solution to the culture medium for 30 minutes on the day of implantation, at a final concentration of 50 μg/ml. Cells were rinsed six times in PBS to remove unbound DAPI. Labeled cells were detached with 0.25% (w/v) trypsin and suspended in serum-free medium for grafting. For instant transplantation after surgical occlusion of the left anterior descending coronary artery, MSCs (2.0×10^5 cells) were suspended in 10 μl serum-free medium and kept on ice until injection with a 30-gauge needle on a Hamilton syringe at three sites, into anterior and lateral aspects of the viable myocardium bordering the infarction. There are five groups of eight rats each used in this study as follows: Normal, non-ligated sham rat; Control, ligated but not implanted rat; MSCs, ligated and MSCs implanted rat; Hph-1-MSCs, ligated and Hph-1 vector only delivered MSCs implanted rat; Hph-1-Hsp70-MSCs: ligated and Hph-1-Hsp70-delivered MSCs implanted rat. Then each group was subdivided three groups of eight rats. One group was injected with DAPI stained MSCs for determining the survival rate of MSCs after 3 days after implantation. MSCs were implanted into the rest two groups, one group was used for morphologic analysis at 1 week, and other for echocardiography at 3 weeks.

Histology and Immunohistochemistry

Transplanted animals were euthanized at 1 week after implantation and their hearts excised, perfusion-fixed with 10% (v/v) neutral buffered formaldehyde for 24 hours, transversely sectioned into four comparable sections, and embedded in paraffin by routine methods. Sections of 2 μm were mounted on gelatin-coated glass slides to allow use of different stains on successive sections of tissue cut through the implantation area. After deparaffinization and rehydration, the sections were stained with hematoxylin and eosin (H&E) to assess nuclei, cytoplasm, and connective tissue. Histological analysis was performed using the manufacturer's instructions (Vector Laboratories, Burlingame, CA, http://www.vectorlabs.com). In brief, excised heart tissues were fixed in 3.7% buffered formaldehyde and embedded in paraffin. Tissue sections of 5 μm were deparaffinized, rehydrated and rinsed with PBS. Antigen retrieval was performed by microwaving for 10 minutes with 10 mM sodium citrate (pH 6.0). Sections were incubated in 3% H_2O_2 to quench endogenous peroxidase. Sample was blocked in 2.5% normal horse serum, and incubated in primary antibody (CD31). Biotinylated pan-specific universal secondary antibody and streptavidin/peroxidase complex reagent were used for the heart sections, which were stained with antibody using a DAB substrate kit. Counterstaining was with 1% methyl green, and dehydration progressed with 100% N-butanol, ethanol and xylene before mounting in VectaMount Medium (Vector Laboratories, Burlingame, CA, http://www.vectorlabs.com). Other serial sections were analyzed with mouse anti-MHC, mouse anti-MLC, and mouse anti-CTnT obtained from Santa Cruz, and rabbit anti-connexin 43 and rabbit anti-N-cadherin from Cell Signaling. FITC-conjugated goat anti-rabbit IgG and Texas red-conjugated goat anti-mouse IgG (Jackson ImmunoResearch, West Grove, PA, http://www.jacksonimmuno.com) were used as secondary antibodies. All images were made using an excitation filter under reflected light fluorescence microscopy and transferred to a computer equipped with MetaMorph software version 4.6 (Universal Imaging Corporation, Downingtown, PA, USA, http://www.moleculardevices.com/pages/software/metamorph.html).

Determination of Infarct Size

TTC staining was used to assess myocardial tissue viability and determine the size of the myocardial infarct. The tissue slices were incubated in a 1% 2, 3, 5-triphenyltetrazolium chloride (TTC, Sigma, St. Louis, MO, http://www.sigma.com) solution, pH 7.4, at 37°C for 20 minutes. The tissues were fixed in 10% PBS-buffered formalin overnight at 2–8°C. The hearts were

sectioned transaxially and the size of myocardial infarction was evaluated as a percentage of the sectional area of the infarcted tissue of the left ventricle to the sectional area of the whole left ventricle. Both sides of each TTC-stained tissue slice were photographed with a digital camera.

Terminal Deoxynucleotidyl Transferase–Mediated dUTP Nick-End Labeling (TUNEL) Assay

TUNEL Assay was performed according to the manufacturer's instructions (Chemicon International Inc., Temecula, CA, http://www.chemicon.com) on excised heart tissues prepared as described above. A positive control sample was prepared from a normal heart section by treating the section with DNase I (10 U/ml, 10 minutes at room temperature). Sections were pretreated with 3.0% H_2O_2, subjected to TdT enzyme for 37°C for 1-hour, and incubated in digoxigenin-conjugated nucleotide substrate at 37°C for 30 minutes. Nuclei exhibiting DNA fragmentation were visualized by adding 3,3-diaminobenzidine (DAB) (Vector Laboratories, Burlingame, CA, http://www.vectorlabs.com) for 5 minutes. The nuclei of apoptotic cells were stained dark brown. Lastly, sections were counterstained with methyl green and sections were observed by light microscopy. For each group, six slices were prepared and ten different regions were observed per slice (× 400).

Assessment of Cardiac Function

Transthoracic echocardiographic studies were performed by an experienced cardiologist blinded to group assignments, at baseline (before LAD ligation), immediately after LAD ligation (before treatment) and 3 weeks after cell transplantation (after treatment) using a GE Vivid Seven ultrasound machine (GE Medical System, Salt Lake City, UT, http://www.gehealthcare.com) with a 10.0 MHz transducer. Rats received general anesthesia and were placed in the left lateral decubitus position. The echo transducer was placed on the left hemithorax and short axis views were recorded. Two-dimensional images were obtained at midpapillary level [20, 21]. M-mode tracing of left ventricular (LV) contraction was obtained at the same level as the short-axis view. LV end diastolic diameter (LVEDD) and LV end systolic diameter (LVESD) were measured with M-mode tracing. Percent fractional shortening (% FS) was determined using [(LVEDD − LVESD)/LVEDD] × 100(%). LV end diastolic volume (LVEDV) was calculated as $7.0 \times \text{LVEDD}^3/(2.4 + \text{LVEDD})$, LV end systolic volume (LVESV) as $7.0 \times \text{LVESD}^3/(2.4 + \text{LVESD})$ and LV ejection fraction (EF) as EF(%) = (LVEDV − LVESV)/LVEDV × 100. Two images per view were obtained and each parameter was measured from three consecutive beats per image. Six values of each parameter were obtained and averaged. Echocardiograms were stored digitally and analyzed with EchoPAC with custom 2-D strain rate imaging software. More than three images were obtained in the short axis view and the parameters were measured from three consecutive beats in each image. For quantitative analysis of regional LV systolic function, peak systolic circumferential strain and peak systolic radial strain were measured on six segments (anteroseptum, anterior, anterolateral, posterolateral, inferior, inferoseptum) of the mid LV level in the parasternal short-axis view. For quantitative analysis of global LV systolic function, the average values of peak systolic circumferential and peak systolic radial strain of the six segments were calculated.

Statistical Analysis

Results are expressed as mean ± SEM. Statistical comparisons between the two groups were performed using the Student's *t* test. In addition, a one-way ANOVA using a Bonferroni test was used when comparing more than two groups. A *p*-value $< .05$ was considered significant.

Results

Kinetics of Hph-1-Hsp70 Delivery into MSCs and Hsp70 Expression Under Hypoxic Conditions

MSCs were isolated from mixed culture with hematopoietic cells based on their attachment to the culture plate, and further purified by exclusion with magnetic beads targeting the hematopoietic marker CD34. Yield was 3×10^6 cells (95% purity) after 2 weeks of culture. Consistent with a previous report [19], the cultured MSCs expressed CD71, CD90, CD105, CD106, and ICAM, but not the hematopoietic markers CD34 and CD14 (data not shown). For direct delivery of Hsp70 protein into MSCs, Hph-1-Hsp70 fusion protein was generated and purified as a single band (data not shown). After pretreatment of MSCs with Hph-1-Hsp70 protein for 1-hour under normal culture conditions, Hph-1-Hsp70 protein was readily delivered into MSCs and detected in the cytoplasm in less than 30 minutes, reaching a maximal intracellular concentration before 120 minutes. The delivery kinetics of Hph-1-Hsp70 were dose- and time-dependent (Fig. 1A). The delivered protein was observed in the cytoplasm and the nucleus, and intracellular Hph-1-Hsp70 protein was observed for more than 12 hours (supporting information Fig. 1B). As demonstrated in our previous report [18], 12 hours of Hph-1 fusion protein in the cells was sufficient to provide over 5 days of in vivo functional effectiveness to a fusion-protein partner. To investigate whether hypoxia modulated Hsp70 in MSCs, cells were exposed to hypoxia for varying periods. Expression of Hsp70 increased after 1-hour of hypoxia, but decreased after 6-hour, and was eventually strongly downregulated (supporting information Fig. 2). These data suggest that the substantial cell death of MSCs following prolonged hypoxia could be due to a decrease in Hsp70 expression.

Anti-Apoptotic Effects of Delivered Hsp70 on MSCs in Hypoxic Conditions

The survival rate of MSCs after 24 hours in hypoxic conditions is normally 70% lower than MSCs cultured in normoxic conditions. Hph-1-Hsp70 treatment enhanced the survival rate of MSCs by about 65% compared to untreated MSCs (Normoxia vs. Hypoxia: 1.09 ± 0.10 vs. 0.32 ± 0.04, $p < .001$; Hph-1-Hsp70 vs. Hypoxia: 0.92 ± 0.06 vs. 0.32 ± 0.04, $p < .001$) (Fig. 1B). In addition, the survival rate after prolonged hypoxic stress (24–72 hours) was higher for Hph-1-Hsp70-treated MSCs than Hph-1-treated MSCs (supporting information Fig. 3). To further confirm the effect of delivered Hph-1-Hsp70 on apoptosis of MSCs under hypoxic conditions, we analyzed the level of caspase-3 activity in MSCs delivered with Hph-1-Hsp70 into after hypoxic incubation. Hypoxia induced a 2.8-fold increase in caspase-3 activity, but activity in Hph-1-Hsp70-treated MSCs was reduced significantly after 24 hours of hypoxia (Normoxia vs. Hypoxia: 0.1 ± 0.01 vs. 0.28 ± 0.05, $p < .001$; Hph-1-Hsp70 vs. Hypoxia: 0.14 ± 0.04 vs. 0.28 ± 0.05, $p < .05$) (Fig. 1C). Depletion of ATP is the earliest cell-damaging factor after ischemic insult. Accordingly, we analyzed the cellular ATP level of MSCs treated with Hph-1-Hsp70 under hypoxic conditions. Hypoxic stress caused a significant decrease in cellular ATP of about 65%, compared to normoxic culture MSCs. Delivery of Hph-1-Hsp70 effectively protected MSCs from ATP depletion under hypoxic conditions (Normoxia vs. Hypoxia: 800 ± 56 vs. 280 ± 16, $p < .001$; Hph-1-Hsp70 vs. Hypoxia: 704 ± 88 vs. 280 ± 16, $p < .001$) (Fig. 1D). In addition, intracellular Hph-1-Hsp70 substantially increased expression of anti-apoptotic protein Bcl-2 and decreased expression of the pro-apoptotic

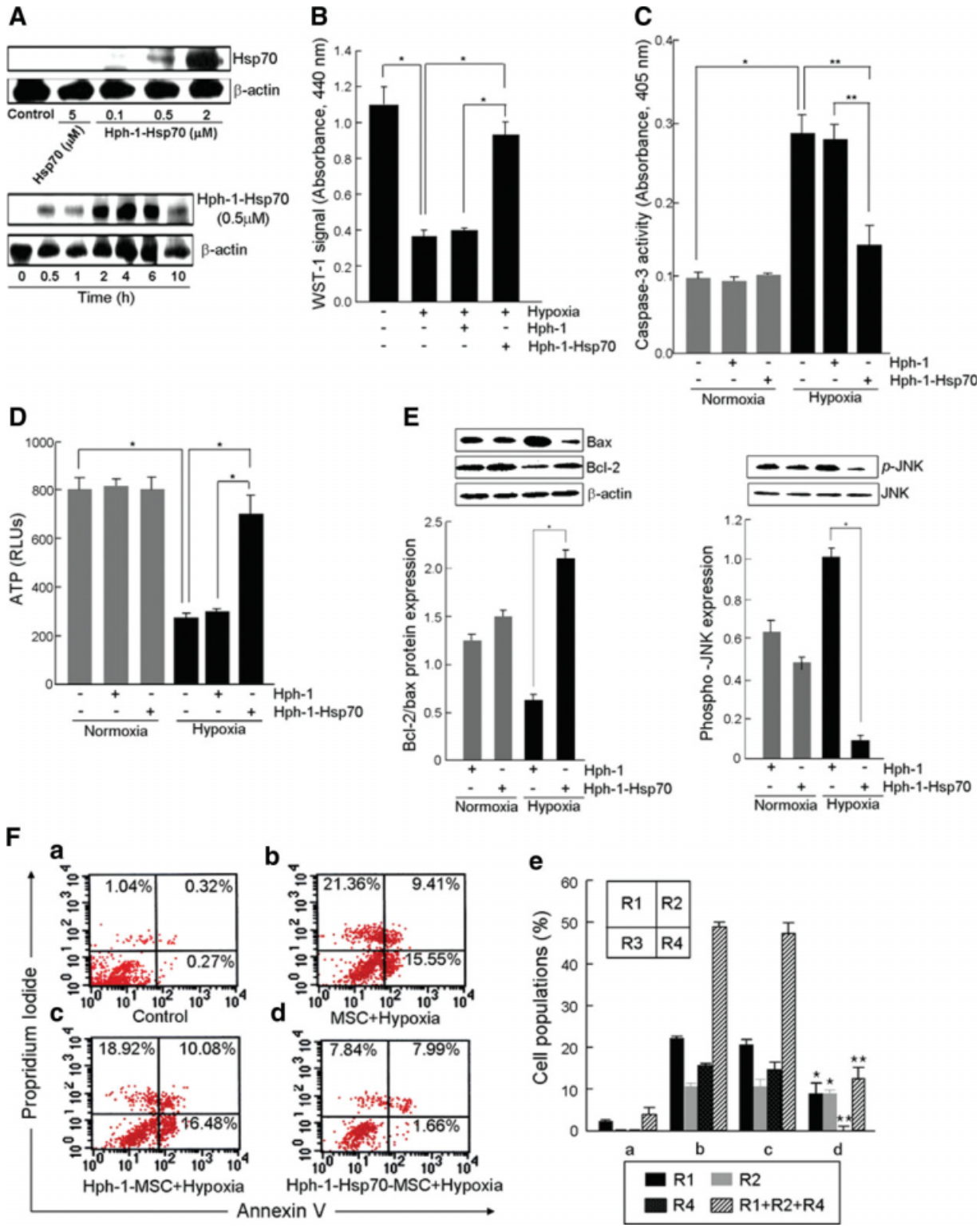

Figure 1. Anti-apoptotic Effects of Delivered Hsp70 on MSCs in Hypoxic Conditions. **(A)** Delivery kinetics of Hph-1-Hsp70 protein into MSCs. MSCs were incubated in 1% FBS DMEM culture medium containing Hph-1-Hsp70 (0.1-2 μM) for 1-hour. The delivered Hsp70 in MSCs was detected by Western blot. **(B)** Viability of MSCs. MSCs (1.5×10^4) were seeded in 96-well plates and cultured for 24 hours. MSCs were treated with 0.5 μM Hph-1-Hsp70 fusion protein and simultaneously exposed to hypoxic or normoxic conditions for 24 hours. WST-1 reagent was added to each well for 3 hours at 37°C. Cell proliferation was measured by spectrophotometry ($\lambda = 570$ nm) (*$p < .001$). **(C)** Caspase-3 activity of MSCs. MSCs (1×10^6) were seeded in 60 mm plates and cultured for 24 hours. MSCs were pretreated with 0.5 μM Hph1-Hsp70 fusion protein followed by 24 hours of hypoxia or normoxia. Caspase-3 activity was measured as described in Materials and Methods (*$p <$ .001, **$p < .05$). **(D)** Intracellular ATP level of MSCs. MSCs (1.5×10^4) were plated into 96-well plates and cultured for 24 hours. After pretreatment with 0.5 μM Hph-1-Hsp70 fusion protein and hypoxic or normoxic incubation for 24 hours, nucleotide-releasing reagent and ATP-monitoring reagent were added into each well, luminescence measured by luminometer (*$p < .001$). **(E)** Apoptosis-related signals in MSCs. MSCs were treated with 0.5 μM Hph-1-Hsp70 and subjected to hypoxia or normoxia. After 6 hours, cells were harvested and β-actin, Bcl-2, Bax, JNK, and phospho-JNK levels determined by immunoblotting (*$p < .001$). **(F)** Representative flow cytometry of annexin V binding versus propidium iodide (PI) uptake **(A–D)** and regional cell percentage **(E)** in MSCs at 24 hours after hypoxia. R1-4 represent the percentage of damaged, necrotic, live, and apoptotic cells, respectively (*$p < .01$ vs. MSC+hypoxia, **$p < .001$ vs. MSC + hypoxia).

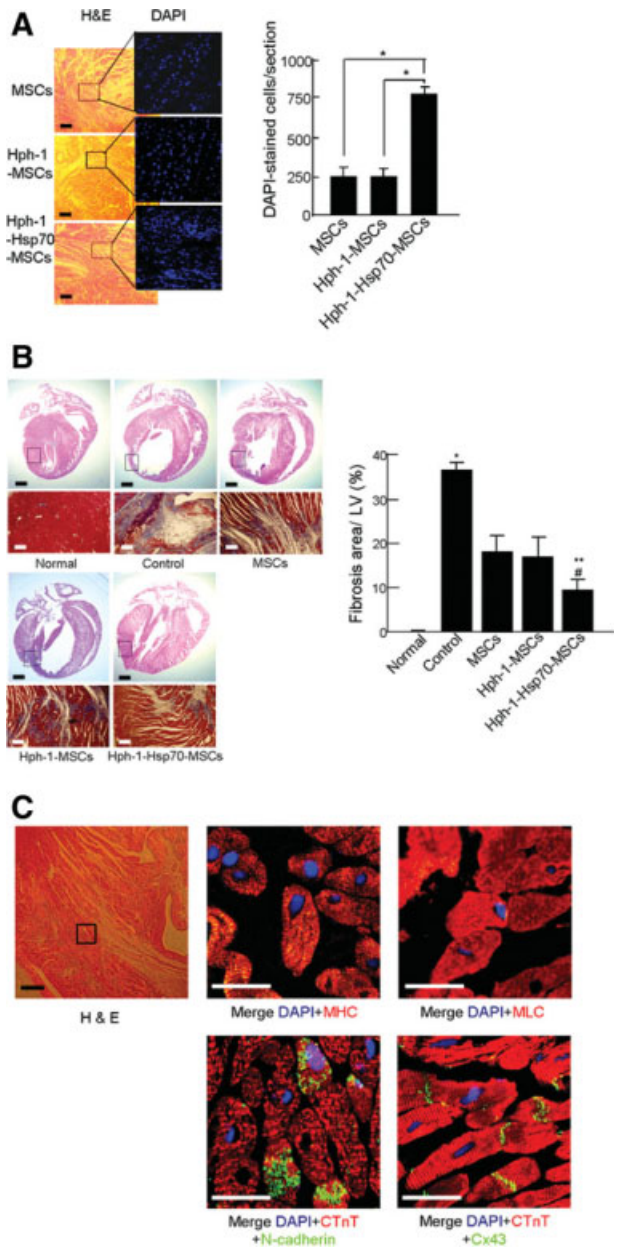

Figure 2. Changes in Representative Histological Sections after Hsp70-MSC Implantation. **(A)** Detection of viable MSCs in ligated hearts by Hph-1-Hsp70 pretreatment. Three days after implantation of DAPI-labeled MSCs into MI-induced animal, DAPI-labeled cells were observed by fluorescence microscope (*$p < .001$). Scale bar: 100 μm. **(B)** Change of morphology in ligated heart by Hph-1-Hsp70 pretreatment. Top panel: Whole heart was harvested 7 days after implantation of MSCs and H&E stained. Bottom panel: Masson's Trichrome stain of the infarcted region showing blue coloration of fibrotic areas, and orange/brown muscle tissue. H&E staining of the infiltration of viable, mature cardiac myocytes from the border zone into the scar area (*$p < .001$ vs. MSCs, $^{\P}p < .05$ vs. MSCs, $^{\#}p < .001$ vs. control). Scale bar: H&E (2 mm), Trichrome: (100 μm). **(C)** Enhanced potential for differentiation and integration of MSCs by Hph-1-Hsp70 pretreatment. DAPI-labeled MSCs on the contact surface with host myocytes were analyzed for cardiac-specific markers cardiac troponin T (cTnT), MHC, MLC, connexin-43 (green), N-cadherin (green), or cTnT (red) by immunohistochemical staining. Scale bar: H&E (150 μm), immunohistological staining: (50 μm).

protein Bax (Hph-1-Hsp70-Hypoxia vs. Hph-1-Hypoxia: 2.4 $\pm$ 0.08 vs. 0.62 $\pm$ 0.09, $p < .001$). Phosphorylation of JNK was also significantly inhibited by Hph-1-Hsp70 (Hph-1-Hsp70-Hypoxia vs. Hph-1-Hypoxia: 0.5 $\pm$ 0.04 vs. One.03 $\pm$ 0.07, $p < .001$) (Fig. 1E). Figure 1F shows a representative analysis and regional percentage of annexin V versus PI dot plot of MSC, with and without Hph-1-Hsp70, in hypoxia or normoxia. After pretreatment with Hph-1-Hsp70, the percentage of damaged, necrotic, and apoptotic cells in the R1, R2, and R4 areas decreased compared to the hypoxia control group (R1. Hypoxia vs. Hph-1-Hsp70: 21.36 $\pm$ 0.36 vs. Seven.84 $\pm$ 0.34, $p < .01$; R2. Hypoxia vs. Hph-1-Hsp70: 9.41 $\pm$ 0.12 vs. Seven.99 $\pm$ 0.21, $p < .01$; R4. Hypoxia vs. Hph-1-Hsp70: 15.55 $\pm$ 0.45 vs. One.66 $\pm$ 0.48, $p < .001$; R1 + R2 + R4. Hypoxia vs. Hph-1-Hsp70: 46.32 $\pm$ 0.47 vs. 17.49 $\pm$ 0.38, $p < .001$). These results demonstrate that delivery of Hph-1-Hsp70 effectively enhances viability of MSCs.

Improved Myocardial Repair After Hsp70-MSC Implantation

To investigate the in vivo therapeutic efficacy of Hph-1-Hsp70-MSCs in myocardial infarction, we transplanted Hph-1-, or Hph-1-Hsp70-MSCs, or MSCs labeled with DAPI into the border region between the infarcted and normal area of the heart after coronary ligation. After 3 days, hearts were removed and the fate of the MSCs was investigated using confocal microscopy. A higher number of Hph-1-Hsp70-MSCs was retained in the border region than control MSCs (Hph-1-Hsp70-MSC vs. MSC: 731 $\pm$ 42 vs. 212 $\pm$ 49, $p <$ .001) (Fig. 2A). In addition, time course experiments indicated enhanced survival of Hph-1-Hsp70-treated MSCs compared to non-treated MSCs (supporting information Fig. 4). One week after coronary ligation, the size of the left ventricular infarct was evaluated in the transplanted and untreated groups. The degree of fibrosis in the infarct zone was substantially higher in MSC-transplanted group than in the Hph-1-Hsp70-MSC-transplanted group (Control vs. MSC: 39.5 $\pm$ 10.39 vs. 18.47 $\pm$ 1.03, $p < .01$; MSC vs. Hph-1-Hsp70-MSC: 18.47 $\pm$ 1.03 vs. Nine.31 $\pm$ 1.67, $p < .05$; control vs. Hph-1-Hsp70-MSC: 39.5 $\pm$ 10.39 vs. Nine.31 $\pm$ 1.67, $p <$ .001) (Fig. 2B). To confirm that the implanted cells had become cardiac myocyte-like cells, cardiac-specific markers were examined by immunohistochemistry. CTnT, MHC, and MLC were detected in the DAPI-positive cells. DAPI-stained Hph-1-Hsp70-MSCs also expressed connexin-43 and N-cadherin in the regions with the host cardiomyocytes, indicating that DAPI-labeled donor cells were well-incorporated into the non-labeled cells (host cardiomyocytes) (Fig. 2C). And, we determined the infarct sizes in the left ventricle (LV) using TTC staining. Injection of Hph-1-Hsp70-MSCs significantly decreased in infarct size compared to MSCs only or Hph-1-MSCs (Control vs. Hph-1-MSC: 29.89 $\pm$ 2.5 vs. 12.43 $\pm$ 2.51, $p < .001$; control vs. Hph-1-Hsp70-MSC: 29.89 $\pm$ 2.5 vs. Six.12 $\pm$ 1.38, $p < .001$; Hph-1-MSC vs. Hph-1-Hsp70-MSC: 12.43 $\pm$ 2.51 vs. Six.12 $\pm$ 1.38, $p < .05$; MSC vs. Hph-1-Hsp70-MSC: 15.03 $\pm$ 1.49 vs. Six.12 $\pm$ 1.38) (Fig. 3A). The incidence of TUNEL-positive myocardial cells was significantly reduced by 19.5 $\pm$ 2.1% in the ligated hearts transplanted with Hph-1-Hsp70-MSCs compared to control (Control vs. Hph-1-Hsp70-MSC: 24.9 $\pm$ 0.9% vs. Five.4 $\pm$ 1.2%, $p < .001$; MSC vs. Hph-1-Hsp70-MSC: 15.8 $\pm$ 2.5% vs. Five.4 $\pm$ 1.2%, $p < .05$) (Fig. 3B). The mean microvessel count per field in the infarcted myocardium was significantly higher in the Hph-1-Hsp70-MSCs group than in other groups (Control vs. Hph-1-Hsp70-MSC: 21 $\pm$ 5 vs. 122 $\pm$ 13, $p <$ .001; MSC vs. Hph-1-Hsp70-MSC: 75 $\pm$ 12 vs. 122 $\pm$ 13,

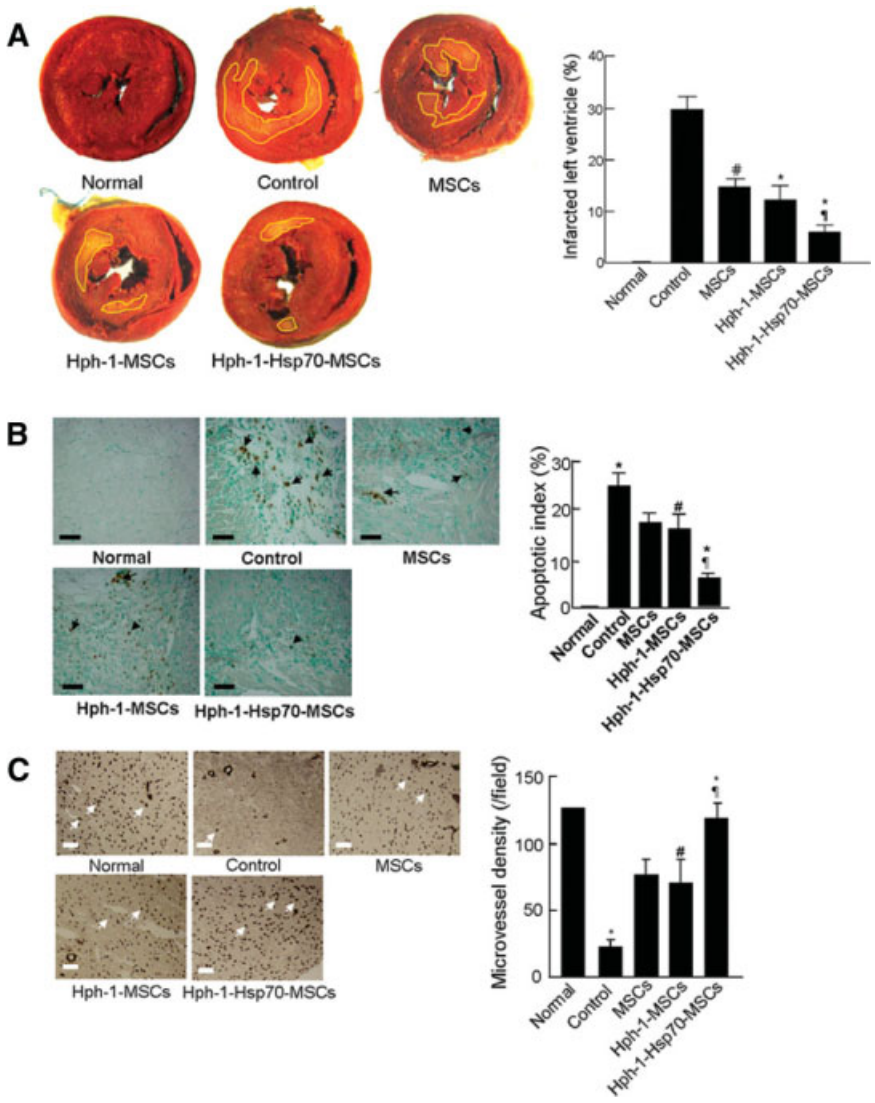

Figure 3. Improved Myocardial Repair after Hsp70-MSC Implantation. **(A)** Intramyocardial injection of MSCs reduced the left ventricular (LV) infarct size as assessed by TTC staining at 7 days post-MI. Hph-1-Hsp70-MSCs further decreased the area of necrotic tissue (*$p < .001$ vs. control, $^{¶}p < .05$ vs. Hph-1-MSCs, $^{\#}p < .001$ vs. Hph-1-Hsp70-MSCs). **(B)** Apoptosis assay on heart tissue, 1 week after LAD ligation. The left panel shows representative TUNEL staining images (magnification: 200×). Staining for normal nuclei (green) using methyl green. Apoptotic nuclei are brown. The right panel shows summarized data from the left panel (*$p < .05$ vs. MSCs, $^{¶}p < .001$ vs. control, $^{\#}p < .01$ vs. Hph-1-MSCs). Scale bar: 100 μm. **(C)** Quantitative analysis with microvessel density significantly higher in Hsp70-MSC groups than in MSC and control groups. Brown: positive staining for CD31 (*$p < .001$ vs. MSCs, $^{¶}p < .05$ vs. control, $^{\#}p < .01$ vs. Hph-1-MSCs). Scale bar: 100 μm.

$p < .05$) (Fig. 3C). To confirm generation of tumor in heart implanted MSCs, cells (2.0×10^4 cells/μl) were directly injected from the injured region to the border using a Hamilton syringe (direct injection in the ventricular wall). There was no tumor formation in heart including other organs (data not shown).

Effective Improvement of Cardiac Function by Implantation of Hph-1-Hsp70-MSCs

To examine the functional improvement fostered by Hph-1-Hsp70-MSCs transplantation, cardiac dimensions and performance parameters were measured by transthoracic echocardiography. At baseline (i.e., after infarction and before cell transplantation), echocardiographic parameters were not significantly different between the control groups. Implantation of MSCs and Hph-1-Hsp70-MSCs showed further improvement in systolic performance (FS of Control vs. Hph-1-Hsp70-MSC: 14.63 ± 2.22 vs. 27.99 ± 3.04, $p < .01$), cardiac dimensions (LVEDV of Control vs. Hph-1-Hsp70-MSC: 0.84 ± 0.07 vs. 0.53 ± 0.08, $p < .01$), and strain (Peak S rad of Control vs. Hph-1-Hsp70-MSC: 3.91 ± 1.07 vs. 20.04 ± 1.84, $p < .01$) compared to control. However, cardiac dimensions including LVEDD (Control vs. Hph-1-Hsp70-MSC: 7.21 ± 0.50 vs. Five.62 ± 0.40, $p < .01$) and LVESD (Control vs. Hph-1-Hsp70-MSC: 6.11 ± 0.38 vs. Three.71 ± 0.36, $p < .01$) were substantially smaller in the Hph-1-Hsp70-MSCs–treated group compared to the MSCs-treated group (Table 1). Transplantation of Hph-1-Hsp70-MSCs resulted in a further increase in systolic performance (37.7% increment in % FS and 28.7% increment in % EF) compared to the MSCs-transplanted group. The peak circumferential and radial strain on the infarct zone and the global circumferential and radial strain were significantly higher in the Hph-1-Hsp70-MSCs group than other groups (Fig. 4).

Discussion

Irreversible tissue damage and physiologic dysfunction occur in the heart as a consequence of myocardial infarction [22]. Recent attempts to repair infarcted hearts using alternative sources of cardiomyocytes revealed that myogenic cells from various stem cells replaced resident myocytes in cardiac tissue after injury [23]. Attempts at postinfarct stem cell

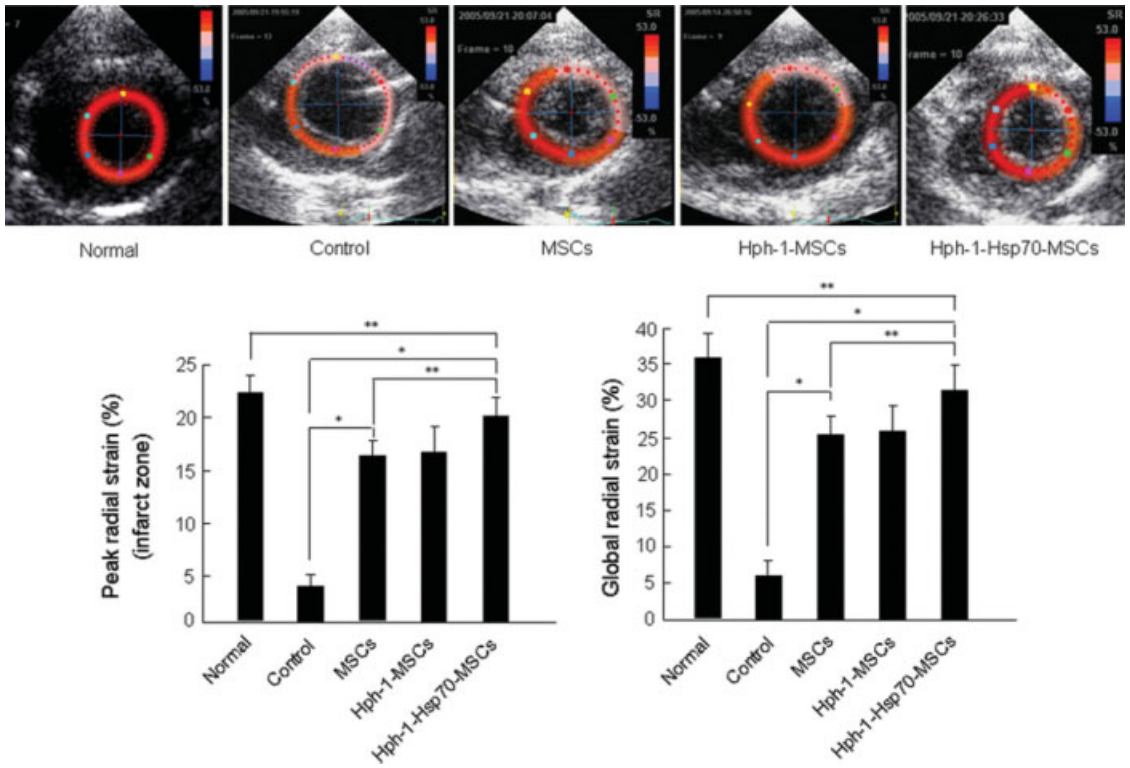

Figure 4. Effective Improvement of Cardiac Function by Implantation of Hph-1-Hsp70-MSCs. Cardiac functions were measured by two-dimensional conventional parameters, fractional shortening (FS), and LV ejection fraction (EF) 3 weeks after injection of MSCs in IM-induced rats. M-mode tracing of LV contraction was obtained at the same level as the short-axis view. LVEDD and LVESD were measured with M-mode tracing. Percent fractional shortening (% FS) was determined as [(LVEDD − LVESD)/LVEDD] × 100(%). LV end diastolic volume (LVEDV) was calculated as 7.0 × $LVEDD^3$/ (2.4 + LVEDD), LV end systolic volume (LVESV) as 7.0 × $LVESD^3$/(2.4 + LVESD) and LV ejection fraction (EF) as EF (%) = (LVEDV − LVESV)/LVEDV × 100 (*$p < .01$, **$p < .05$).

Table 1. Echo-data for untreated control, MSCs-treated, Hph-1-MSCs, and Hph-1-Hsp70-MSCs- treated rats

Variables	Normal ($n = 8$)	Control ($n = 8$)	MSCs ($n = 8$)	Hph-1-MSCs ($n = 8$)	Hph-1-Hsp70-MSCs ($n = 8$)
LVEDD (mm)	5.51 ± 0.31	7.21 ± 0.50	6.72 ± 0.52[a]	6.64 ± 0.48[a]	5.62 ± 0.40[a,b,c,d]
LVESD (mm)	3.31 ± 0.22	6.11 ± 0.38	5.35 ± 0.50[a]	5.28 ± 0.29[a]	3.71 ± 0.36[a,b,c,d]
FS (%)	39.64 ± 5.54	14.63 ± 2.22	20.33 ± 1.95[a]	20.15 ± 2.90[a]	33.98 ± 3.04[a,b,c,d]
LVEDV (ml)	0.43 ± 0.03	0.84 ± 0.07	0.69 ± 0.19[a]	0.66 ± 0.10[a]	0.53 ± 0.08[a,b,c,d]
LVESV (ml)	0.17 ± 0.03	0.54 ± 0.08	0.37 ± 0.12[a]	0.35 ± 0.09[a]	0.21 ± 0.07[a,b,c,d]
LVEF (%)	68.5 ± 6.1	35.5 ± 4.8	47.0 ± 3.7[a]	46.7 ± 5.3[a]	60.5 ± 4.1[a,b,c,d]
Peak S cir (%) (infarct zone)	−7.81 ± 1.14	−1.90 ± 0.40	−4.31 ± 1.72[a]	−4.79 ± 1.20[a]	−6.60 ± 1.25[a,d,e,f]
Peak S rad (%) (infarct zone)	24.23 ± 1.92	3.91 ± 1.07	16.33 ± 1.40[a]	16.97 ± 1.97[a]	20.04 ± 1.84[a,b,c,d]
Global S cir (%)	−20.32 ± 1.64	−4.23 ± 1.63	−7.64 ± 1.27[a]	−8.10 ± 2.31[a]	−12.05 ± 1.40[a,d,e,f]
Global S rad (%)	38.23 ± 4.42	5.58 ± 2.42	25.14 ± 3.65[a]	26.00 ± 3.81[a]	31.81 ± 3.75[a,d,e,f]

Values are mean ± S.D.
[a]$p < 0.01$ vs. control, [b]$p < 0.05$ vs. MSCs, [c]$p < 0.05$ vs. Hph-1-MSCs, [d]$p < 0.05$ vs. normal, [e]$p < 0.01$ vs. MSCs, [f]$p < 0.01$ vs. Hsp70-SCs.
Abbreviations: LVEDD, left ventricular end diastolic diameter; LVESD, left ventricular end systolic diameter; FS, fractional shortening; LVEDV, left ventricular end diastolic volume; LVESV, left ventricular end systolic volume; MSCs, mesenchymal stem cells; S cir, circumferential strain; S rad, radial strain.

transplantation therapy in the myocardium show a poor rate of survival, however [24]. Cell death is influenced by an ischemic environment that is devoid of nutrients and oxygen [12], coupled with the loss of survival signals because of inadequate interaction between cells and matrix [25]. Recently, enhancing the viability of MSCs by introduction of the Akt survival signal was used as a new approach in the early post-transplant period, and resulted in improvement in the regeneration of infarcted myocardium [13].

Heat shock protein (Hsp) is synthesized transiently as a tool to protect cellular homeostasis after exposure to heat and potentially deleterious stimuli. Hsp70 also inhibits apoptosis in a caspase-independent manner [26]. This is likely to involve Hsp70 inhibition of JNK, which plays a key role in

inducing apoptotic cell death in response to specific stimuli [27, 28]. Mechanistic studies in non-cardiac cells on the inhibiting effect of Hsp70 on pro-apoptotic mechanisms parallel the direct demonstration that over-expression of Hsp70 can inhibit apoptosis in implanted MSCs [9].

Despite accumulating evidence on the protective role of Hsp70, many problems remain in direct gene delivery to the heart for cardiac protection, similar to all gene therapy procedures [9, 15, 16, 29]. As described above, genetic manipulation of cells by transfection or viral introduction of cDNA expression vectors and microinjection of proteins into cells presents various difficulties, including low transfection efficiency and cytotoxicity from chemical agents and harmful viral transfection [15–17]. In this study, we synthesized Hsp 70 fusion proteins with Hph-1-PTD, a peptide capable of freely transducing bound proteins into cells. TAT, an HIV-derived PTD that can cross cell membranes, was discovered in 1988 by two independent groups [30, 31]. Our previous report identified a novel cell-permeable PTD from the human transcriptional factor Hph-1, and successfully delivered Hph-1-PTD immunosuppressive proteins in vivo and in vitro through different administration routes, for the treatment of various autoimmune diseases [18]. This work on myocardial repair aims to overcome the problem of cell death after implantation by improving cell viability with MSCs delivered with Hph-1-Hsp70.

Hph-1-Hsp70-MSCs showed a remarkable increase in survival under hypoxic conditions. In addition, we observed that JNK phosphorylation, caspase-3 and pro-apoptotic Bax decreased significantly. We also confirmed increases in levels of anti-apoptotic Bcl-2. Any form of cell injury, as well as ischemia, results in a rapid decrease in cytoplasmic ATP levels. Kabakov et al. [32] reported that Hsp70 overexpression attenuates proteotoxicity of cellular ATP depletion. We also observed that delivery of Hph-1-Hsp70 attenuated ATP depletion in MSCs under hypoxic conditions. After pretreatment with Hph-1-Hsp70, the percentage of damaged, necrotic, and apoptotic cells decreased compared to the hypoxia control group. According to our in vivo histological findings, transplantation of Hph-1-Hsp70-MSCs resulted in a further decrease in infarct size and improvement of microvessel density. Indeed, improvement in cardiac structure was related with reduction of fibrotic area and infarct size, higher capillary density. Especially, Hph-1-Hsp70-MSCs-mediated increase in microvessel formation may increase blood flow within the infarcted area and contribute to inhibition of cardiac remodeling, and subsequent improvement in systolic function. Moreover, transplantation of Hph-1-Hsp70-MSCs into infarction-induced animals significantly improved heart function assessed by various parameters. Neither cytotoxic effects on MSCs with significantly higher concentrations of Hph-1-Hsp70 nor tumorigenesis of Hph-1-Hsp70-treated MSCs were detected (data not shown), and behavioral abnormalities were not observed in mice implanted with Hph-1-Hsp70-MSCs. According to transthoracic echocardiography, transplantation of Hph-1-Hsp70-MSCs was decreased in LV chamber size, and improved LV systolic function. These functional parameters of the heart showed functional and structural improvement following Hph-1-Hsp70-MSCs transplantation.

Conclusion

In this report, we demonstrate that modification of MSCs by Hph-1-Hsp70 effectively protected MSCs from in vitro and in vivo cell death caused by different mechanisms of apoptosis under hypoxic conditions, leading to improved MSC cell viability. Hph-1-Hsp70-MSCs retained function in the infarcted region of the myocardium and promoted the expression of cardiac-specific markers on MSCs. Transplantation of Hph-1-Hsp70-MSCs into infarction-induced animals significantly improved LV function, limited LV remodeling, and changed heart structure after myocardial infarction assessed by various parameters. Our results suggest that enhancing the viability and integration potential of MSCs by Hph-1-Hsp70 treatment before transplantation provides novel therapeutic opportunities for the treatment of myocardial infarction and end-stage cardiac failure.

Acknowledgments

This research was supported by a Korea Science and Engineering Foundation (KOSEF) Grant funded by MOST (M1064102000106N410200110); a grant (SC-2150) from Stem Cell Research Center of 2first Century Frontier Research Program funded by the Ministry of Education, Science and Technology, Republic of Korea and by the Korea Science; and a grant from the Korea Health 21 R&D Project, Ministry of Health & Welfare, Republic of Korea A085136).

Disclosure of Potential Conflicts of Interest

Ki-Chul Hwang owns stock in Yonsei University and Dong-Ho Lee, Ki-Doo Choi, and Seung-Kyou Lee all served as officers or members of the board for ForHuman-Tech Co.

References

1 Makino S, Fukuda K, Miyoshi S et al. Cardiomyocytes can be generated from marrow stromal cells in vitro. J Clin Invest 1999;103: 697–705.
2 Shake JG, Gruber PJ, Baumgartner WA et al. Mesenchymal stem cell implantation in a swine myocardial infarct model: Engraftment and functional effects. Ann Thorac Surg 2002;73:1919–1925.
3 Toma C, Pittenger MF, Cahill KS, Byrne BJ, Kessler PD. Human mesenchymal stem cells differentiate to a cardiomyocyte phenotype in the adult murine heart. Circulation 2002;105:93–98.
4 Jäättelä M. Heat shock proteins as cellular lifeguards. Ann Med 1999; 31:261–271.
5 Latchman DS. Heat shock proteins and cardiac protection. Cardiovasc Res 2001;51:637–646.
6 Beere HM, Green DR. Stress management–heat shock protein-70 and the regulation of apoptosis. Trends Cell Biol 2001;11:6–10.
7 Höhfeld J. Regulation of the heat shock conjugate Hsc70 in the mammalian cell: The characterization of the anti-apoptotic protein BAG-1 provides novel insights. Biol Chem 1998;379:269–274.
8 Kiang JG, Tsokos GC. Heat shock protein 70 kDa: Molecular biology, biochemistry, and physiology. Pharmacol Ther 1998;80:183–201.
9 Brar BK, Stephanou A, Wagstaff MJ et al. Heat shock proteins delivered with a virus vector can protect cardiac cells against apoptosis as well as against thermal or hypoxic stress. J Mol Cell Cardiol 1999;31: 135–146.
10 Gray CC, Amrani M, Yacoub MH. Heat stress proteins and myocardial protection: Experimental model or potential clinical tool. Int J Biochem Cell Biol 1999;31:559–573.
11 Okubo S, Wildner O, Shah MR, Chelliah JC, Hess ML, Kukreja RC. Gene transfer of heat-shock protein 70 reduces infarct size in vivo after ischemia/reperfusion in the rabbit heart. Circulation 2001;103:877–881.

12 Zhang M, Methot D, Poppa V, Fujio Y, Walsh K, Murry CE. Cardiomyocyte grafting for cardiac repair: Graft cell death and anti-death strategies. J Mol Cell Cardiol 2001;33:907–921.
13 Mangi AA, Noiseux N, Kong D et al. Mesenchymal stem cells modified with Akt prevent remodeling and restore performance of infarcted hearts. Nat Med 2003;9:1195–1201.
14 Würtele H, Little KC, Chartrand P. Illegitimate DNA integration in mammalian cells. Gene Ther 2003;10:1791–1799.
15 Martin JL, Mestril R, Hilal-Dandan R, Brunton LL, Dillmann WH. Small heat shock proteins and protection against ischemic injury in cardiac myocytes. Circulation 1997;96:4343–4348.
16 Suzuki K, Sawa Y, Kaneda Y, Ichihara H, Shirakura R, Matsuda H. In vivo gene transfection with heat shock protein 70 enhances myocardial tolerance to ischemia-reperfusion injury in rat. J Clin Invest 1997; 99:1645–1650.
17 Anderson WF. Human gene therapy. Nature 1998;392:25–30.
18 Choi JM, Ahn MH, Chae WJ et al. Intranasal delivery of the cytoplasmic domain of CTLA-4 using a novel protein transduction domain prevents allergic inflammation. Nat Med 2006;12:574–579.
19 Song H, Chang W, Lim S et al. Tissue transglutaminase is essential for integrin-mediated survival of bone marrow-derived mesenchymal stem cells. Stem Cells 2007;25:1431–1438.
20 Langeland S, D'hooge J, Wouters PF et al. Experimental validation of a new ultrasound method for the simultaneous assessment of radial and longitudinal myocardial deformation independent of insonation angle. Circulation 2005;112:2157–2162.
21 Nagaya N, Kangawa K, Itoh T et al. Transplantation of mesenchymal stem cells improves cardiac function in a rat model of dilated cardiomyopathy. Circulation 2005;112:1128–1138.
22 Ho KK, Anderson KM, Kannel WB et al. Survival after the onset of congestive heart failure in Framingham Heart Study subjects. Circulation 1993;88:107–115.
23 Davani S, Deschaseaux F, Chalmers D et al. Can stem cells mend a broken heart?Cardiovasc Res 2005;65:305–316.
24 Guérette B, Skuk D, Celestin F et al. Prevention by anti-LFA-1 of acute myoblast death following transplantation. J Immunol 1997;159:2522–2531.
25 Meredith JE, Jr Fazeli B, Schwartz MA. The extracellular matrix as a cell survival factor. Mol Biol Cell 1993;4:953–961.
26 Jäättelä M, Wissing D, Kokholm K, Kallunki T, Egeblad M. Hsp70 exerts its anti-apoptotic function downstream of caspase-3-like proteases. EMBO J 1998;17:6124–6134.
27 Gabai VL, Yaglom JA, Volloch V et al. Hsp72-mediated suppression of c-Jun N-terminal kinase is implicated in development of tolerance to caspase-independent cell death. Mol Cell Biol 2000;20:6826–6836.
28 Park HS, Lee JS, Huh SH, Seo JS, Choi EJ. Hsp72 functions as a natural inhibitory protein of c-Jun N-terminal kinase. EMBO J 2001;20: 446–456.
29 Meldrum DR, Meng X, Shames BD et al. Liposomal delivery of heat-shock protein 72 into the heart prevents endotoxin-induced myocardial contractile dysfunction. Surgery 1999;126:135–141.
30 Green M, Loewenstein PM. Autonomous functional domains of chemically synthesized human immunodeficiency virus tat trans-activator protein. Cell 1988;55:1179–1188.
31 Frankel AD, Pabo CO. Cellular uptake of the tat protein from human immunodeficiency virus. Cell 1988;55:1189–1193.
32 Kabakov AE, Budagova KR, Latchman DS et al. Stressful preconditioning and HSP70 overexpression attenuate proteotoxicity of cellular ATP depletion. Am J Physiol Cell Physiol 2002;283:C521–C534.

See www.StemCells.com for supporting information available online.